JOURNAL OF SPACECRAFT AND ROCKETS
Vol. 40, No. 3, May–June 2003

Design and Optimization of Low-Thrust Trajectories with Gravity Assists

T. Troy McConaghy,* Theresa J. Debban,† Anastassios E. Petropoulos,‡ and James M. Longuski§
Purdue University, West Lafayette, Indiana 47907-1282

Missions such as Mariner 10, Voyager 1, Galileo, and Stardust all used gravity-assist flybys to achieve their mission goals efficiently. Methods to design such gravity-assist missions are fairly well developed and generally assume all major maneuvers are performed impulsively by chemical rockets. The recent success of the low-thrust Deep Space 1 mission demonstrates that low-thrust (high-efficiency) propulsion is ready to be used on future missions, potentially reducing the required propellant mass or the total time of flight. By combining both gravity-assist flybys and low-thrust propulsion, future missions could enjoy the benefits of both. To realize such missions, an effective design methodology is needed. A two-step approach to the design and optimization of low-thrust gravity-assist trajectories is described. The first step is a search through a broad range of potential trajectories. To speed up this search, a simplified shape-based trajectory model is used. The best trajectories are chosen using a heuristic cost function. The second step optimizes the most promising trajectories using an efficient parameter optimization method. Examples of missions designed using this approach are presented, including voyages to Vesta, Tempel 1, Ceres, Jupiter, and Pluto.

Nomenclature

g	=	standard acceleration due to gravity, m/s^2
I_{sp}	=	engine specific impulse, s
k_0	=	scale factor for exponential sinusoid, astronomical units (AU)
k_1	=	dynamic range parameter for exponential sinusoid
k_2	=	winding parameter for exponential sinusoid, rad^{-1}
$\dot{m}$	=	engine mass flow rate, mg/s
P	=	engine input power, kW
p_{mf}	=	low-thrust propellant mass fraction
R_J	=	radius of Jupiter
r	=	distance from central body, AU
T	=	engine thrust, mN
t_{mf}	=	total propellant mass fraction
V_∞	=	hyperbolic excess speed, km/s
ΔV	=	magnitude of change in velocity, km/s
θ	=	polar (clock) angle, rad
ϕ	=	phase angle for exponential sinusoid, rad

Introduction

IN the 1950s and 1960s, the idea of using planetary flybys for gravity assists became widely known.[1–5] Such flybys were shown to enable otherwise impossible missions in the solar system. However, until 5 February 1974, the interplanetary gravity assist was an untested idea. On that day, now a generation ago, Mariner 10 used a gravity assist at Venus to achieve the first close flyby of Mercury. Thus began a new era in which the gravity-assist maneuver became and continues to be a trusted and useful technique for enabling deep-space exploration.

Another technology, solar electric propulsion (SEP), has only recently proven its worthiness for interplanetary missions. In March 2001, the ion propulsion system[6] on Deep Space 1 (DS1), produced jointly by the NASA Solar Electric Propulsion Technology Application Readiness program and the New Millennium Program DS1 program, exceeded 10,000 h of operation in interplanetary space. The specific impulse I_{sp} of this thruster is about 10 times that of chemical rockets, enabling large savings in propellant costs. The increased I_{sp} comes at the cost of low thrust, but that is offset by the ability to thrust for long durations. Used together, gravity-assist maneuvers and low-thrust propulsion permit a new type of trajectory that we refer to as a low-thrust gravity-assist (LTGA) trajectory. The LTGA concept provides a means to shorten mission duration and reduce propellant requirements. For example, missions to Pluto can have their time of flight (TOF) reduced from 12 to 9 years by using low thrust instead of chemical propulsion.[7,8] Similarly, rendezvous missions to Jupiter can have their launch energy and total propellant requirements reduced.[8] Unfortunately, designing LTGA trajectories is a formidable task. Unlike ballistic trajectories, optimal low-thrust arcs are not simple geometric shapes (as are conic sections). In fact, there are infinitely many possible low-thrust arcs between any two target bodies (even for a given time of flight). The task is further complicated by timing, that is, phasing, considerations, especially when the trajectory involves multiple gravity assists. Because of the difficulties currently faced when designing LTGA trajectories, no commonly accepted approach has yet emerged. Other researchers have proposed various methods and applied them to the design of missions ranging from Mercury orbiters to heliopause explorers.[7,9–25] In this paper, we describe a new two-step method that combines a broad-search technique developed by Petropoulos et al.[26] with a parameter optimization program based on the work of Sims and Flanagan.[27] The broad search capitalizes on a shape-based scheme to represent LTGA trajectories. The optimization approach represents trajectories as a series of impulsive maneuvers and conic arcs.

Methodology

Step 1: Broad Search

The first step of our methodology is the evaluation of a broad range of LTGA trajectories. The goal is to find many good but different trajectories, each of which can then be improved by a local optimizer (in step 2).

To reduce the time needed to evaluate each LTGA trajectory (and increase the number that we can consider), we avoid time-consuming numerical propagation. To do this, we assume a

Received 25 March 2002; revision received 3 December 2002; accepted for publication 12 December 2002.

*Ph.D. Candidate, School of Aeronautics and Astronautics. Student Member AIAA.

†Graduate Student, School of Aeronautics and Astronautics; currently Member of the Engineering Staff, Navigation and Mission Design Section, Mail Stop 301-140L, Jet Propulsion Laboratory, California Institute of Technology, Pasadena, CA 91109-8099. Member AIAA.

‡Ph.D. Candidate, School of Aeronautics and Astronautics; currently Senior Member of the Engineering Staff, Navigation and Mission Design Section, Mail Stop 301-140L, Jet Propulsion Laboratory, California Institute of Technology, Pasadena, CA 91109-8099. Member AIAA.

§Professor, School of Aeronautics and Astronautics. Associate Fellow AIAA.

two-body model and patch together coast and thrust arcs. We employ conic sections for the coasting arcs and "exponential sinusoids"[26] for the thrusting arcs. Exponential sinusoids are planar geometric curves that are given in polar coordinates r and θ by

$$r = k_0 \exp[k_1 \sin(k_2\theta + \phi)] \quad (1)$$

where k_0, k_1, k_2, and ϕ are constants. Once the trajectory shape is specified, the thrust acceleration required at each point is completely determined if tangential thrust (either along or against the velocity vector) is assumed.[28] Thus, we make this tangential thrust assumption so that no differential equations need to be propagated numerically in the patched-arc model. Instead, we propagate the trajectories analytically. These LTGA trajectories are constructed simply by solving transcendental equations and quadratures. Such computationally fast calculations enable the rapid evaluation of many trajectories.

The mathematical and algorithmic details of this first step are worked out by Petropoulos et al.,[26] Petropoulos and Longuski,[29,30] and Petropoulos.[28] Petropoulos and Longuski implemented the algorithms[29,30] as an extension of STOUR (see Ref. 31). When setting up a search in STOUR, we begin by choosing the sequence of bodies to be visited. Then we decide where to apply coast and thrust arcs. STOUR provides four options for the path between each pair of bodies: 1) a pure thrust arc, 2) a pure coast arc, 3) a coast/thrust arc, or 4) a thrust/coast arc. In the latter two cases, we also specify 1) the distance from the central body, for example, the sun, at which the engine may switch between on and off and 2) the permitted spacecraft radial velocity direction(s) (in or out) at the point where the switch occurs.

Most of the parameters in STOUR have default values. Thus, for a simple problem, a user need only specify the path, the launch date and launch V_∞ ranges, the step sizes, and the maximum total time of flight. Other user-specified STOUR parameters include maximum time of flight on each leg, for example, Earth to Mars, maximum arrival V_∞, maximum k_1 value, maximum propellant mass fraction, maximum propellant mass fraction for in-plane thrusting, and engine I_{sp} (which we assume to be constant). Power availability constraints are not set explicitly, but can be enforced implicitly by specifying a maximum thrust acceleration (either in meters per second squared or in local solar gs, the gravitational acceleration due to the sun). A maximum can also be specified for the average thrust acceleration. For each leg involving thrust, there exists a one-parameter family of solutions. Because explicit solutions are not available, sampling of the family requires a numerical search over two parameters, taken as k_2 and the V_∞ turn angle. The coarseness of the search is controlled by setting step sizes for the k_2 parameter and the V_∞ turn angle.

Generally, we desire rendezvous missions with low arrival V_∞, low propellant mass fraction, and low time of flight for a given launch V_∞. For flyby missions, the arrival V_∞ magnitude is less important. STOUR often finds several thousand trajectories that meet the requirements and constraints. To rank these solutions, we use a heuristic cost function that we call the total propellant mass fraction t_{mf}, which accounts for the launch V_∞, the arrival V_∞ (in the case of a rendezvous), and STOUR's thrust arc propellant mass fraction (the ratio of propellant mass to initial spacecraft mass). (Note that we do not consider spiraling trajectories about the launch or the destination body.) The launch V_∞ is converted to a mass fraction via Tsiolkovsky's rocket equation[32] (also see Ref. 33) as if it were a ΔV. We use a chemical I_{sp} of 350 s, I_{sp1}, for the launch. For the arrival V_∞, we assume an optimizer would eliminate the excess velocity over the course of the low-thrust arc. Therefore, we employ the rocket equation with an I_{sp} of 3000 s, I_{sp2}, typical for highly efficient low-thrust engines.[6] Combining these two factors with the propellant mass fraction of the thrust arc, p_{mf}, the total propellant mass fraction t_{mf} is calculated using

$$t_{mf} = 1 - (1 - p_{mf}) \exp(-V_{\infty 1}/g I_{sp1}) \exp(-V_{\infty 2}/g I_{sp2}) \quad (2)$$

where $V_{\infty 1}$ is the launch V_∞ and $V_{\infty 2}$ is the arrival V_∞. For flyby missions, we drop the second exponential factor. The t_{mf} is understood to be a rough estimate of the cost of a trajectory, that is, its name should not be taken too literally.

The TOF, though important, is not included in the cost function t_{mf}, and so we evaluate a trajectory's total propellant mass fraction together with its time of flight. Even though several trajectories may have similar low t_{mf}, they may have rather different characteristics. For example, their launch V_∞ or their launch dates may differ significantly. Thus, the mission designer may wish to choose several candidates for optimization in step 2.

Step 2: Optimization

We optimize candidate LTGA trajectories found in step one using a direct method developed by Sims and Flanagan.[27] Their approach produced results comparable to SEPTOP,[20] a well-tested optimization tool that uses the calculus of variations.

In the Sims–Flanagan[27] LTGA trajectory model, each leg of the trajectory is subdivided into segments of equal duration. (A leg connects two mission bodies, such as an Earth–Mars leg.) The thrusting on each segment is modeled by an impulse at the midpoint of the segment, with conic arcs between the impulses. (In this aspect, the Sims–Flanagan model is similar to that used by Kawaguchi et al.[34]) To ensure that the spacecraft encounters both the initial and final bodies on each leg, the first part of the leg is propagated forward from the initial body and the last part of the leg is propagated backward from the final body. For the trajectory to be feasible, the forward- and backward-propagated partial legs must meet at a "matchpoint," which is often, but not necessarily, at the midpoint of the leg (Fig. 1). This matchpoint problem can be stated as a constraint for the optimizer.

A gravity-assist maneuver is modeled as an instantaneous rotation of $\boldsymbol{V}_\infty$. The magnitude and direction of the rotation are determined by the flyby periapsis altitude and the B-plane angle. The B-plane angle[35] is the angle between $\boldsymbol{T}$ (a vector parallel to the ecliptic plane) and $\boldsymbol{B}$ (the vector from the gravitating center to the target point).

The LTGA trajectory model uses the following variables: 1) the impulsive $\Delta\boldsymbol{V}$ on each segment, 2) the Julian dates at the launch, flyby, and destination bodies, 3) the launch $\boldsymbol{V}_\infty$, 4) the incoming inertial velocity vectors at all of the postlaunch bodies, 5) the spacecraft mass at each body, 6) the flyby periapsis altitude at the gravity-assist bodies, and 7) the B-plane angle at the gravity-assist bodies. These variables can be altered by an optimizer to find the trajectory with the largest mass at the final body. (Note that the optimizer works with normalized variables that all have an order of magnitude close to unity.) Some constraints are imposed to make the resulting trajectory flyable. First, the position, velocity, and mass of the spacecraft must be continuous across the matchpoint on each leg. (This is the matchpoint problem described earlier.) Second, the ΔV magnitude on each segment must not exceed a certain value. This maximum value depends on the spacecraft mass and the available engine power, which in turn depends on the distance of the spacecraft from the sun.

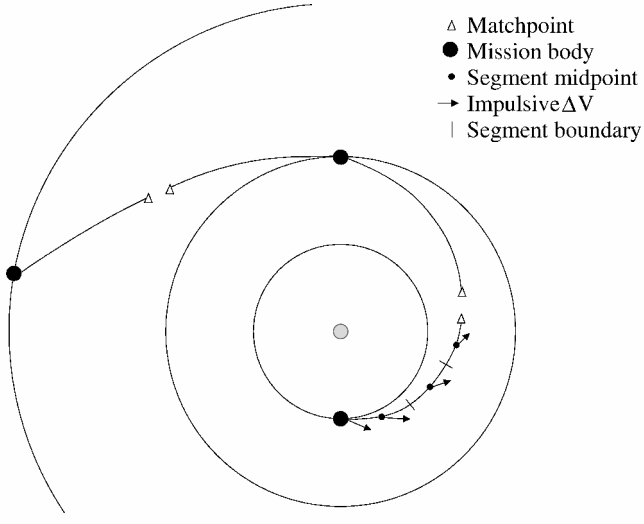

Fig. 1 LTGA trajectory model (after Sims and Flanagan[27]): △, matchpoint; ●, mission body; •, segment midpoint; →, impulsive ΔV; and |, segment boundary.

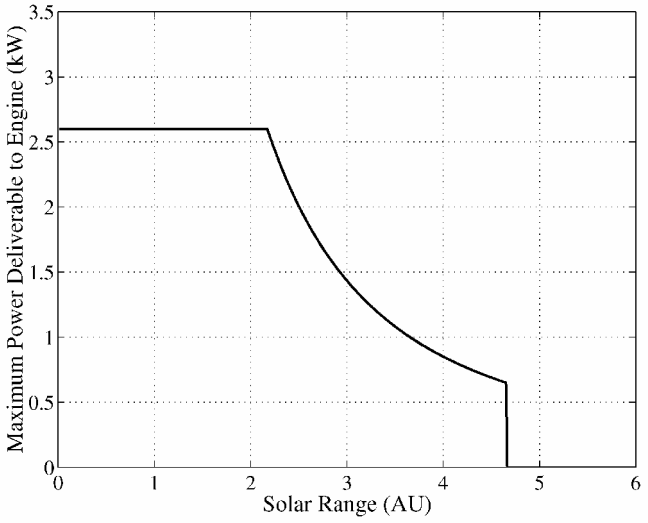

Fig. 2 Power input to ion engine; total array power available at 1 AU is 10 kW.

We can add other mission constraints very easily. For example, if we want a rendezvous with the destination body, we constrain the V_∞ of arrival to be zero. We can also constrain the direction of the launch $\boldsymbol{V}_\infty$ (because in a real launch the $\boldsymbol{V}_\infty$ is constrained by the inclination and ascending node of the low Earth parking orbit, the injection point, and the launch date), but we do not do so for the examples presented in this paper.

The optimization software uses a solar array model that takes into account both the distance from the sun and the effect of temperature on solar cell efficiency. The same model is used by Williams and Coverstone-Carroll.[7] For most of the missions in this paper, we assume that the solar arrays produce 10 kW of power at 1 astronomical unit (AU). (The Earth–Mars–Ceres rendezvous mission is the only exception.) Unless otherwise noted, we also assume that the housekeeping power required by the spacecraft is negligible.

We assume that each low-thrust engine needs at least 0.649 kW of power to operate and can use at most 2.6 kW (the values used by Sims and Flanagan[27] in their original code). Figure 2 shows how the maximum power deliverable to the engine depends on the distance from the sun. The engine thrust and mass-flow rate are modeled as linear functions of the input power, with the coefficients being the same as those used by Williams and Coverstone-Carroll[7]:

$$T = -1.9137 + 36.242P \tag{3}$$

$$\dot{m} = 0.47556 + 0.90209P \tag{4}$$

The engine I_{sp} (in seconds) can be calculated from the thrust and mass-flow rate using

$$I_{sp} = 1000T/g\dot{m} \tag{5}$$

where g is the standard acceleration of gravity ($9.80665 m/s^2$). From the thrust and mass-flow-rate models given in Eqs. (3) and (4), we note that the I_{sp} increases with the input power. Because we want the engine to operate at the maximum possible efficiency, we assume the engine always receives the maximum usable power. When operated at 2.6 kW (which is often the case), the engine I_{sp} is 3337 s. The ΔV achieved on each segment can vary between zero and a maximum value that depends on the mass of the spacecraft, the length of the segment, and the maximum usable power on that segment. This range of ΔV is achieved by varying the thrust duration (not the input power). A single engine is used for all missions considered in this paper.

We use NPOPT for the optimization. NPOPT comes bundled with SNOPT.[36] NPOPT uses a sequential quadratic programming algorithm with an augmented Lagrangian merit function. The user can supply analytically calculated first derivatives of the objective and constraint functions. Otherwise, NPOPT estimates derivatives using finite differences. In our earlier work,[37] we did not calculate all first derivatives analytically, but we do now. We find that, with all first derivatives calculated analytically, we can allow the Julian dates to be free variables and the optimizer will still converge to an optimal solution. (Before the incorporation of the analytic derivatives, allowing dates to be free usually resulted in unconverged results.) We also observe more reliable and robust convergence in general.

Verification of the Optimization Software

Our optimization software, GALLOP, is based heavily on the original Sims and Flanagan[27] code. Nonetheless, GALLOP's code was entirely written by us and, thus, required careful testing. Verification was accomplished by optimizing test cases and comparing the results to results from other software.

One of our test cases is a 2009 Earth–Mars–Vesta flyby mission that was investigated by Sims and Flanagan.[27] The launch V_∞ is fixed at 2.8 km/s. If we assume that the launch vehicle is a Delta 7326-9.5 (the vehicle that launched DS1), then this launch V_∞ implies an initial spacecraft wet mass of 545 kg. The launch, flyby, and arrival dates are fixed at 4 October 2009, 2 May 2010, and 27 January 2011, respectively. We use 26 segments on the Earth–Mars leg and 38 segments on the Mars–Vesta leg. (Consequently, each segment has a duration close to 8 days.)

We compare the optimal solution found by GALLOP to the optimal solution found by two other optimizers: SEPTOP and SDC. SDC uses a new optimization method that is currently being developed.[38] Both SEPTOP and SDC use a numerically integrated trajectory model. The optimized final mass found by GALLOP is 493.73 kg. The Sims and Flanagan[27] software finds precisely the same value (493.73 kg). SEPTOP finds a trajectory with a final mass of 493.74 kg (Ref. 27). SDC finds a trajectory with a final mass of 494.05 kg. A comparison of trajectory characteristics found by the three optimizers is given in Table 1.

Figures 3 and 4 show the solar-system path of the optimal trajectories found by GALLOP and SDC, respectively. The vectors on the GALLOP trajectory (Fig. 3) indicate the direction and relative magnitude of the impulsive ΔV at the midpoint of each segment. The arrows on the SDC trajectory (Fig. 4) indicate the direction and relative magnitude of the instantaneous thrust. Note that in both the

Table 1 Comparison of results from three optimizers for an Earth–Mars–Vesta flyby mission[27]

Optimization software	Final mass, kg	Mars flyby altitude,[a] km	Launch $V_{\infty x}$, km/s	Launch $V_{\infty y}$, km/s	Launch $V_{\infty z}$, km/s
SEPTOP[b]	493.74	2818	−0.810	2.651	0.397
SDC[b]	494.05	2815	−0.808	2.648	0.420
GALLOP	493.73	2838	−0.799	2.651	0.416

[a] Assuming a Mars radius of 3397 km.
[b] SEPTOP and SDC both use numerically integrated trajectories.

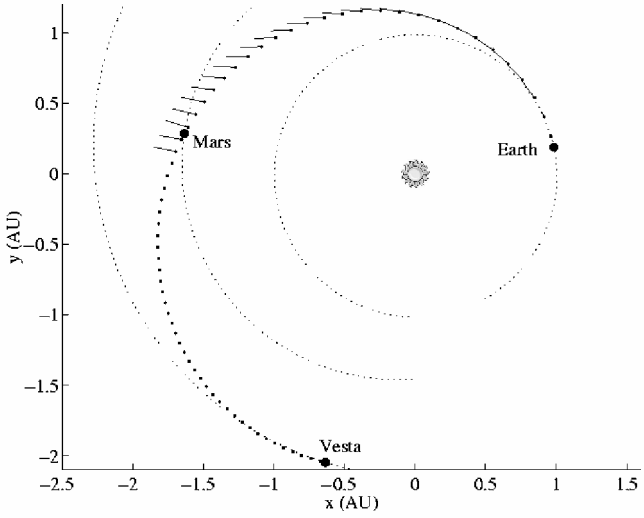

Fig. 3 Mass-optimal Earth–Mars–Vesta flyby trajectory found by GALLOP using impulsive ΔV, patched conic model.

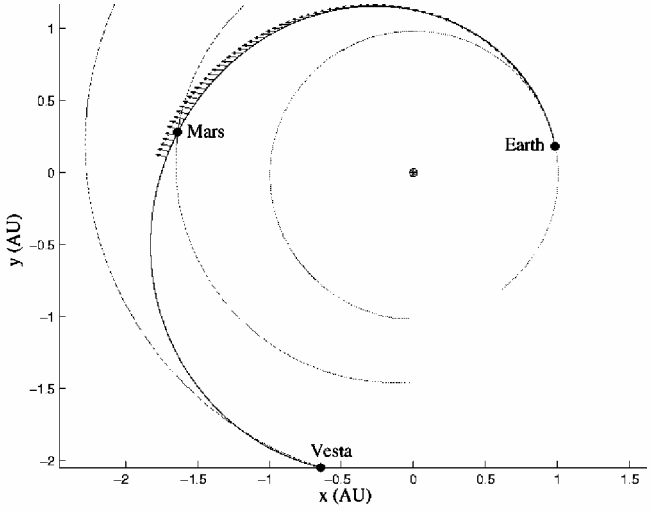

Fig. 4 Mass-optimal Earth–Mars–Vesta flyby trajectory found by SDC using numerically integrated model.

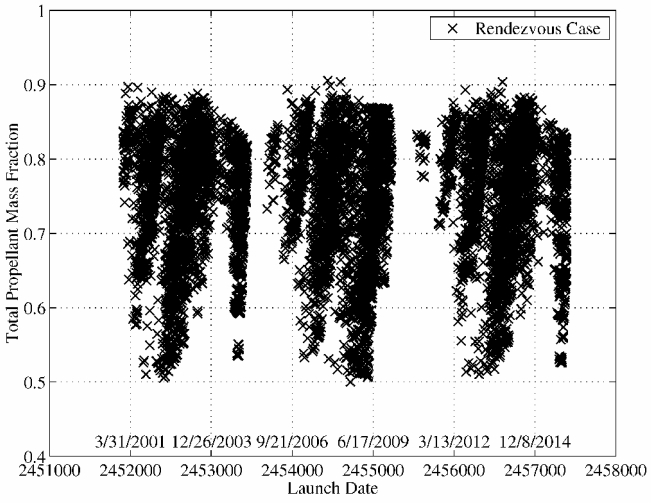

Fig. 5 Low-thrust trajectories to Tempel 1; launch dates between 1 January 2001 and 3 January 2016.

GALLOP and the SDC solutions, the engine thrusts continuously from Earth to Mars and also for a short time after the Mars flyby. The spacecraft then coasts the rest of the way to Vesta. The direction and magnitude of the thrust are in very close agreement in the two solutions. Also note that the propellant used in the two solutions is about the same (50.95 kg in the SDC solution vs 51.27 kg in the GALLOP solution).

The good agreement found with the Earth–Mars–Vesta flyby test case is representative. In general, we found similar agreement between the optimal solutions found by GALLOP and those found by other software for a number of different test cases, for example, an Earth–Mars flyby, an Earth–Mars rendezvous, and an Earth–Mars–Vesta rendezvous. Such agreement shows that, although GALLOP uses a lower-fidelity trajectory model, it is still very accurate.

Numerical Examples

Rendezvous with Comet Tempel 1

Although our tools were created for designing missions with multiple gravity assists, we wanted to find out how well they work for designing direct missions. We consider a direct mission that would rendezvous with Tempel 1. Designing such a mission is challenging due to the high inclination and eccentricity of Tempel 1 (currently 10.5 deg and 0.519, respectively).

We began by using STOUR to perform a broad search for trajectories between 1 January 2001 and 3 January 2016 (Julian dates 2451910–2457390). Figure 5 shows how the total propellant mass fraction (including launch, thrusting, and rendezvous propellant costs) depends on launch date. Each × in Fig. 5 corresponds to a different trajectory.

We see that there are three main groups of trajectories in the range of launch dates considered. For convenience, we will refer to them as group 1, group 2, and group 3, with group 1 having the earliest launch dates and group 3 the latest. Each group of "good" trajectories occurs around a time when Tempel 1 is closest to the sun, that is, near perihelion. Because Tempel 1 has a period of about 5.5 years, a group of good trajectories occurs about every 5.5 years.

Our next step was to take three trajectories from the STOUR run (one from each group) and to use them as initial guesses for optimization in GALLOP. The launch and arrival dates were allowed to be free variables, and the initial spacecraft mass was calculated using the launch V_∞ (also free), assuming a Medlite launch vehicle. The resulting optimized trajectories are shown in Figs. 6–8. The optimized launch dates for group 1, 2, and 3 trajectories are 28 November 2002, 8 April 2009, and 3 December 2013, respectively.

When we compare Fig. 6 to Fig. 8, we notice that the optimized trajectory in group 1 is almost identical to the optimized trajectory in group 3. This is possible because the group 3 trajectory occurs almost exactly 11 years after the group 1 trajectory. Because Earth and Tempel 1 return to the same inertial positions

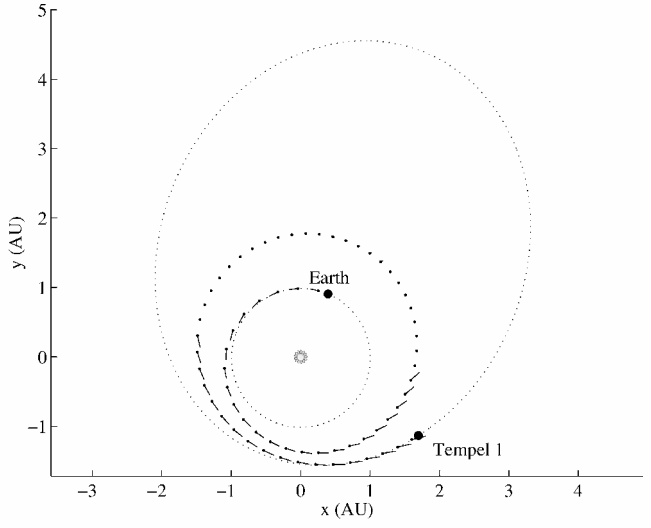

Fig. 6 Mass-optimal Earth–Tempel 1 trajectory from group 1: final mass = 387 kg, TOF = 3 years, and launch V_∞ = 0.8 km/s.

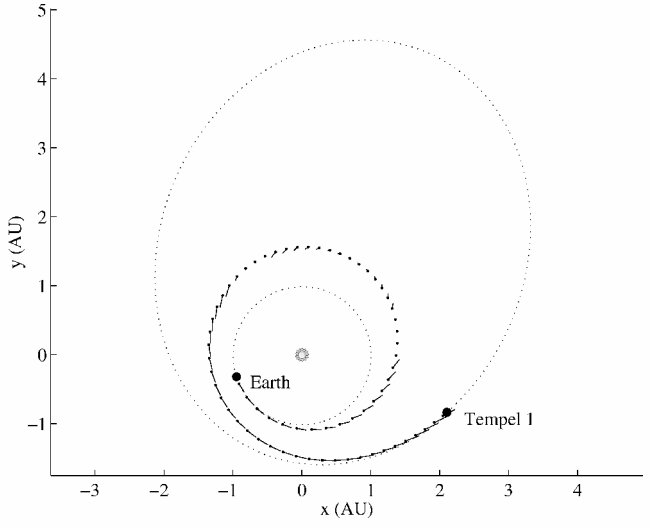

Fig. 7 Mass-optimal Earth–Tempel 1 trajectory from group 2: final mass = 385 kg, TOF = 2.3 years, and launch V_∞ = 1.2 km/s.

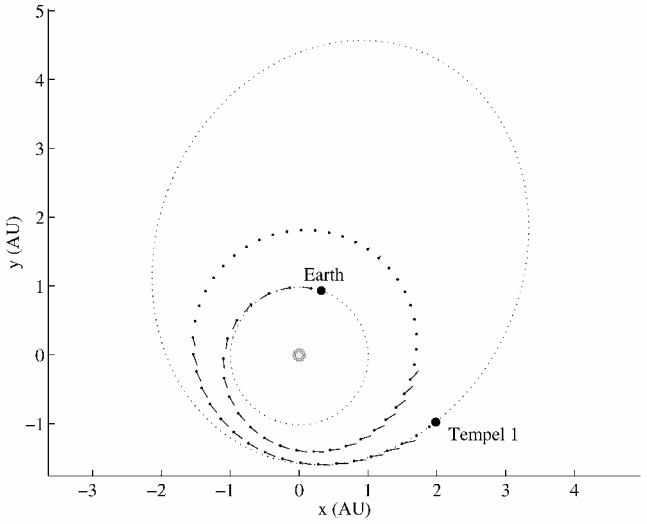

Fig. 8 Mass-optimal Earth–Tempel 1 trajectory from group 3: final mass = 388 kg, TOF = 3.2 years, and launch V_∞ = 0.9 km/s.

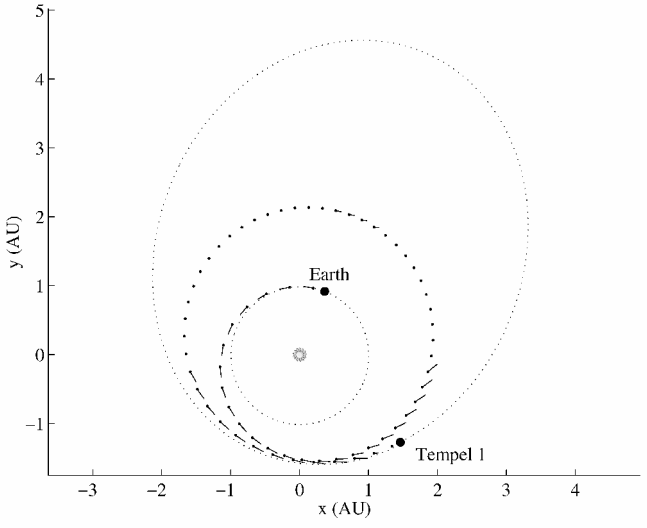

Fig. 9 Mass-optimal Earth–Tempel 1 trajectory from group 2: final mass = 380 kg, TOF = 3.5 years, and launch V_∞ = 1.3 km/s.

every 11 years, every trajectory connecting them must recur every 11 years.

Note that the three optimal solutions shown in Figs. 6–8 (one from each group) are not the only optimal solutions within those groups. An example of a different (locally) optimal solution from group 2 is shown in Fig. 9. The optimized launch date of this trajectory is 1 December 2007. A comparison of Figs. 6, 8, and 9 reveals that all three of these trajectories have a similar shape.

For a specific launch vehicle (a Medlite), we can study how the maximum mass deliverable to Tempel 1 depends on the launch date and arrival date. Figure 10 shows the results of such a study for trajectories in group 3 (launch dates in 2014). For each of the three arrival dates shown in Fig. 10, there is an optimal launch date (which can be found by GALLOP by fixing the arrival date but allowing the launch date to be free). We find that if the arrival date is moved later, the optimal launch date moves earlier, so the optimal time of flight becomes longer. In Fig. 10, the trajectory with the highest deliverable mass (a mass of 364 kg) launches 28 April 2014 and arrives 9 September 2016 and has a TOF of 2.4 years. Optimal trajectories arriving later have a larger mass at Tempel 1, but they have the disadvantage of a longer flight time.

Rendezvous with Ceres via Mars

When the low-thrust version of STOUR was first created, it was tested by checking whether it would find some of the optimized

Table 2 Earth–Mars–Ceres rendezvous trajectory

Characteristic	STOUR/GALLOP	Sauer[20]
Solar array power at 1 AU, W	5.0 kW	5.0 kW
Launch date	6 May 2003	May 2003[a]
Launch V_∞, km/s	1.35	1.35
Initial mass, kg	568	568
Mars flyby altitude, km	200[b]	N/A[c]
Mars flyby V_∞, km/s	1.9 km/s	N/A[c]
Total TOF, yr	3.1	3.0
Final mass, kg	412	410

[a]Exact date not available in Ref. 20.
[b]On lower bound.
[c]Not available in Ref. 20.

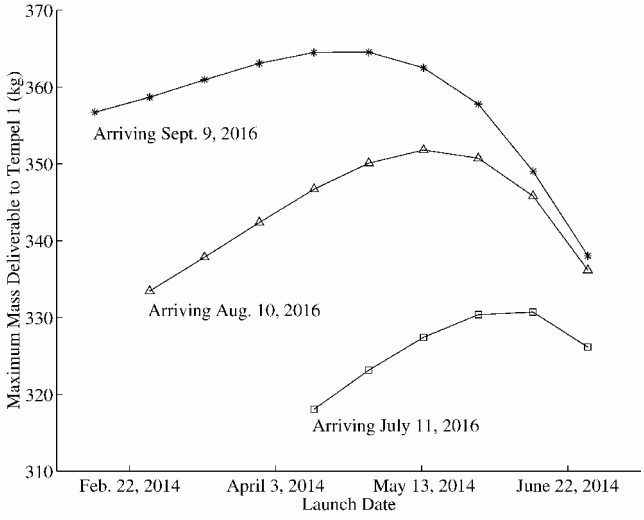

Fig. 10 Maximum mass deliverable to Tempel 1 depending on launch and arrival dates.

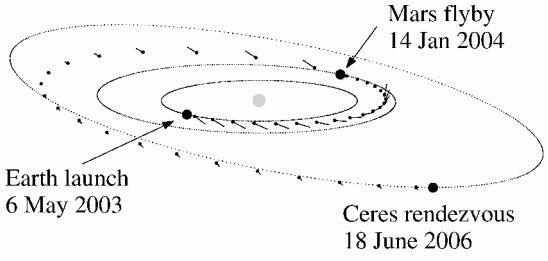

Fig. 11 Earth–Mars–Ceres rendezvous trajectory.

LTGA trajectories in the literature. One such trajectory, by Sauer,[20] performs a gravity-assist maneuver at Mars and ends with a rendezvous at the asteroid Ceres. When STOUR does a broad search for Earth–Mars–Ceres rendezvous trajectories between 1999 and 2040 (Refs. 28–30), the best launch date it finds is within days of the trajectory from Sauer.[20]

The most promising Earth–Mars–Ceres trajectory found by STOUR was used as an initial guess for GALLOP. The launch V_∞ magnitude and initial mass were held fixed at Sauer's[20] values. The spacecraft housekeeping power was assumed to be 125 W, and the minimum power needed to operate the engine was assumed to be 0.5 kW (the values used by Sauer). Table 2 summarizes the pertinent characteristics of the resulting optimized trajectory, which is in good agreement with the result found by Sauer. Note that we did not allow the optimizer to vary the launch V_∞ magnitude or the initial mass. Figure 11 shows a three-dimensional view of the spacecraft trajectory. The direction and relative magnitude of the impulsive ΔV are indicated by line segments emanating from the segment midpoints.

Low-Thrust Mission to Jupiter with Three Intermediate Flybys

One of the special capabilities of STOUR is its ability to find LTGA trajectories with multiple gravity-assist maneuvers, that is,

Table 3 EVEMJ flyby trajectory

Characteristic	Value
Solar array power at 1 AU	10 kW
Number of NSTAR engines	1
Launch date	1 Oct. 2029
Launch V_∞	2.00 km/s
Initial wet spacecraft mass	300.0 kg
Venus flyby date	20 March 2030
Venus flyby V_∞	5.20 km/s
Venus flyby altitude	15448 km
Venus flyby B-plane angle[a]	−68.9 deg
Earth flyby date	13 Jan. 2031
Earth flyby V_∞	8.23 km/s
Earth flyby altitude	300 km[b]
Earth flyby B-plane angle[a]	−176.0 deg
Mars flyby date	13 May 2031
Mars flyby V_∞	15.82 km/s
Mars flyby altitude	200 km[b]
Mars flyby B-plane angle[a]	−9.3 deg
Jupiter flyby date	9 June 2033
Jupiter flyby V_∞	6.04 km/s
Total TOF	1347 days (3.7 yr)
Final dry spacecraft mass	271.7 kg
Propellant mass fraction	0.094

[a] Fundamental plane taken as ecliptic of J2000 (1 January 2000 at 12:00 universal time).
[b] On lower bound.

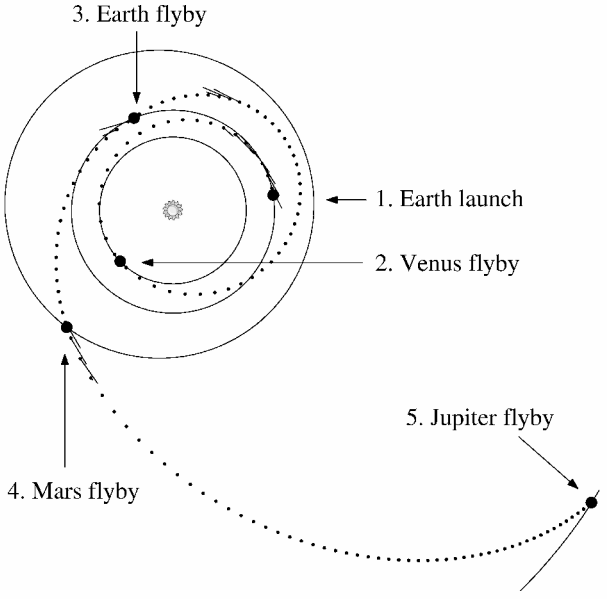

Fig. 12 EVEMJ flyby trajectory.

more than two. For example, a successful search for Earth–Venus–Earth–Mars–Jupiter (EVEMJ) flyby trajectories was conducted by Petropoulos[28] and Petropoulos and Longuski.[30]

We select the EVEMJ trajectory with the lowest in-plane propellant mass fraction for optimization. As with the Earth–Mars–Ceres trajectory, the initial mass and launch V_∞ magnitude are held fixed, but all dates are free. The details of the resulting optimized trajectory are summarized in Table 3.

Figure 12 shows the optimized EVEMJ flyby trajectory, and Fig. 13 shows how the spacecraft specific energy varies during the course of the mission. "Conic Arc" on the horizontal axis of Fig. 13 refers to the sequence number of the conic sections connecting the impulsive ΔV at the segment midpoints (Fig. 1). Note that there are four distinct thrusting phases on the optimized EVEMJ flyby trajectory (which are evident in Fig. 12 and most clearly shown in Fig. 13). The first thrusting phase, occurring immediately after launch, increases the inclination and lowers the energy. The second thrusting phase, occurring shortly after apoapsis on the Venus–Earth leg, decreases the inclination and increases the energy. The third thrusting phase, occurring just after the Venus flyby, increases the energy. The fourth thrusting phase, occurring before and after

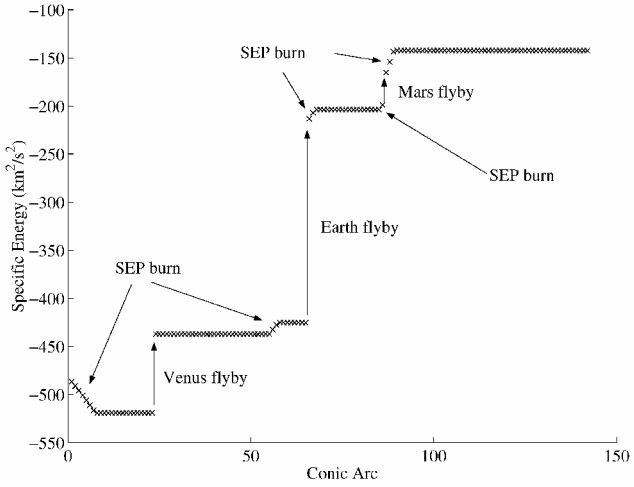

Fig. 13 Energy variation on the EVEMJ flyby trajectory.

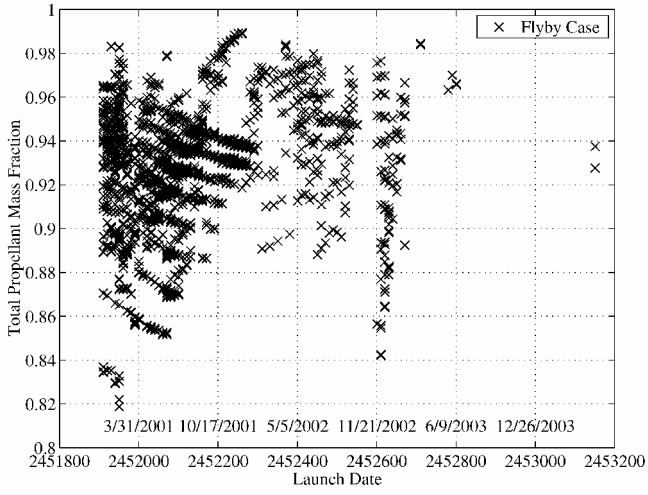

Fig. 14 EVJP trajectories (launch dates between 1 January 2001 and 25 May 2004).

the Mars flyby, increases both the energy and the inclination. Note that the majority of the total energy change is accomplished by the gravity-assist maneuvers at Venus, Earth, and Mars.

Low-Thrust Trajectories to Pluto via Venus and Jupiter

We now consider low-thrust trajectories to Pluto using gravity-assist maneuvers at Venus and Jupiter. It is known that there are Earth–Venus–Jupiter–Pluto (EVJP) trajectories[7,8] for launch in 2004, but we wish to find earlier opportunities where the literature provides no known solutions.

The results of a broad search for such trajectories are shown in Fig. 14. The search spans launch dates between 1 January 2001 and 25 May 2004 (Julian dates 2451910 to 2453150). Because there is no rendezvous at Pluto, the total propellant mass fraction t_{mf} includes only the launch and thrust-leg propellant costs. Note that the majority of trajectories found by STOUR occur in 2001.

There is a promising group of low-thrust EVJP trajectories occurring in late 2002, that is, with low t_{mf} and low time of flight (TOF). We choose one of these trajectories to optimize with GALLOP. The launch V_∞ can be varied, and the initial spacecraft mass is calculated assuming a Delta 7326-9.5 launch vehicle. If the launch date and Pluto arrival date are held fixed (so that the TOF is 12.1 years), we find that the optimal trajectory has a propellant mass fraction of 0.426. When we allow GALLOP to vary all dates freely, the resulting optimal solution has a propellant mass fraction of 0.408, but a very long flight time: 41.2 years. We find that putting an upper bound on the Pluto arrival date reduces the TOF but increases the propellant mass fraction.

Table 4 EVJP flyby trajectory

Characteristic	Value
Solar array power at 1 AU	10 kW
Number of NSTAR engines	1
Launch date	11 May 2002
Launch V_∞	4.98 km/s
Launch vehicle	Delta 7326-9.5
Initial wet spacecraft mass	361.1 kg
Venus flyby date	2 May 2003
Venus flyby V_∞	8.12 km/s
Venus flyby altitude	300 km[a]
Venus flyby B-plane angle[b]	−171.3 deg
Jupiter flyby date	28 Jan. 2005
Jupiter flyby V_∞	12.48 km/s
Jupiter flyby altitude	285968 km ($4R_J$)[a]
Jupiter flyby B-plane angle[b]	7.4 deg
Pluto flyby date	19 Sept. 2012
Pluto flyby V_∞	17.15 km/s
Total TOF	3784 days (10.4 yr)
Final dry spacecraft mass	180.3 kg
Propellant mass fraction	0.501

[a]On lower bound. [b]Fundamental plane taken as ecliptic of J2000 (1 January 2000 at 12:00 universal time).

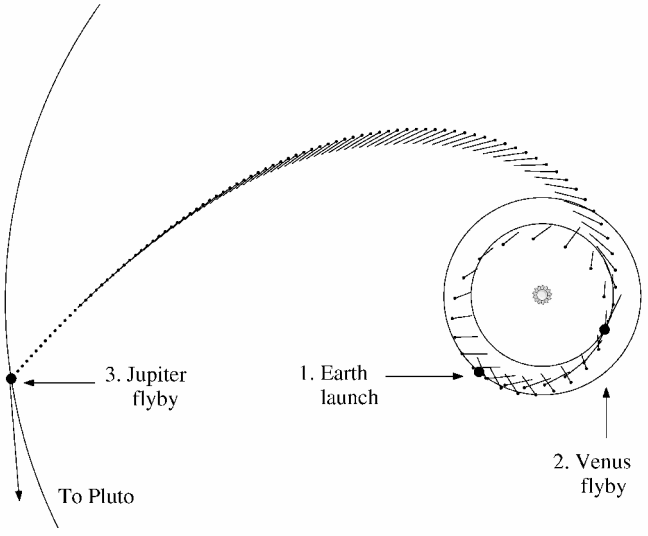

Fig. 15 EVJP trajectory.

Table 4 is a summary of the characteristics of an optimized trajectory where the Pluto arrival date is constrained to be on or before 19 September 2012. (This date is chosen to keep the total time of flight around 10 years.) The TOF is 10.4 years, and the propellant mass fraction is 0.501. Figure 15 shows the first two legs of this trajectory (up to the Jupiter flyby). We note that, on the optimized trajectory, the engine operates at maximum thrust from launch, through the Venus flyby, and until the spacecraft reaches about 4.5 AU. The spacecraft then coasts to the Jupiter gravity assist, which puts the spacecraft on a ballistic trajectory to Pluto. Our discovery of these Pluto trajectories is an encouraging result because it demonstrates the synergistic capabilities of STOUR and GALLOP to find trajectories during launch windows different from those reported in the literature.

Conclusions

We develop a new approach to the difficult problem of designing and optimizing LTGA trajectories. Such trajectories are useful because they can offer reduced TOF or reduced propellant requirements compared to missions using chemical propulsion. Our approach has two steps. First, we perform a broad search for promising trajectories. To speed up this broad search, we use an assumed-shape model for all thrusting and coasting arcs. Each trajectory is evaluated using a heuristic cost function. The best trajectories are selected for step two in which we optimize each candidate trajectory using an efficient parameter optimization method. Our approach has several advantages. The broad-search capability gives the mission designer a global view of the design space, which often contains disparate families of promising trajectories. Also, the optimizer is very fast, thereby enabling quick studies of changes in launch date, arrival date, or launch energy. We hope that our approach will find use in the general problem of LTGA trajectory design and that it will open new doors to the exploration of the solar system.

Acknowledgments

This work has been supported in part by the Jet Propulsion Laboratory (JPL), California Institute of Technology, under Contracts 1211514 and 1223406 (G. T. Rosalia, Contract Manager; and D. V. Byrnes, Technical Manager). The second author acknowledges fellowships provided by NASA Graduate Student Researchers Program Grant NGT5-50275 (JPL Technical Advisor D. V. Byrnes) and the William Koerner Aerospace Foundation. We are grateful to J. Sims and G. Whiffen for providing useful information, guidance, and helpful suggestions. We thank J. Sims and S. Flanagan for providing their optimization code. We also thank G. Whiffen for providing Fig. 4 and the SDC results in Table 1. The optimization software NPOPT (used by GALLOP) is commercially available from Stanford Business Software Inc.

References

[1]Crocco, G. A., "One-Year Exploration Trip Earth-Mars-Venus-Earth," *Proceedings of the VIIth International Astronautical Congress*, Associazione Italiana Razzi, Rome, 1956, pp. 201–252.

[2]Battin, R. H., "The Determination of Round-Trip Planetary Reconnaissance Trajectories," *Journal of the Aero/Space Sciences*, Vol. 26, No. 9, 1959, pp. 545–567.

[3]Breakwell, J. V., Gillespie, R. W., and Ross, S., "Researches in Interplanetary Transfer," *ARS Journal*, Vol. 31, No. 2, 1961, pp. 201–208.

[4]Ross, S., "A Systematic Approach to the Study of Nonstop Interplanetary Round Trips," American Astronautical Society, AAS Paper 63-007, Jan. 1963.

[5]Minovich, M. A., "The Determination and Characteristics of Ballistic Interplanetary Trajectories under the Influence of Multiple Planetary Attractions," Jet Propulsion Lab., JPL TR 32-464, California Inst. of Technology, Pasadena, CA, Oct. 1963.

[6]Brophy, J. R., Kakuda, R. Y., Polk, J. E., Anderson, J. R., Marcucci, M. G., Brinza, D., Henry, M. D., Fujii, K. K., Mantha, K. R., Stocky, J. F., Sovey, J., Patterson, M., Rawlin, V., Hamley, J., Bond, T., Christensen, J., Cardwell, H., Benson, G., Gallagher, J., Matranga, M., Bushway, D., "Ion Propulsion System (NSTAR) DS1 Technology Validation Report," Jet Propulsion Lab., JPL Publ. 00-10, California Inst. of Technology, Pasadena, CA, Oct. 2000.

[7]Williams, S. N., and Coverstone-Carroll, V., "Benefits of Solar Electric Propulsion for the Next Generation of Planetary Exploration Missions," *Journal of the Astronautical Sciences*, Vol. 45, No. 2, 1997, pp. 143–159.

[8]Debban, T. J., McConaghy, T. T., and Longuski, J. M., "Design and Optimization of Low-Thrust Gravity-Assist Trajectories to Selected Planets," AIAA Paper 2002-4729, Aug. 2002.

[9]Meissinger, H. F., "Earth Swingby—A Novel Approach to Interplanetary Missions Using Electric Propulsion," AIAA Paper 70-1117, Aug.–Sept. 1970.

[10]Atkins, L. K., Sauer, C. G., and Flandro, G. A., "Solar Electric Propulsion Combined with Earth Gravity Assist: A New Potential for Planetary Exploration," AIAA Paper 76-807, Aug. 1976.

[11]Sauer, C. G., "Solar Electric Earth Gravity Assist (SEEGA) Missions to the Outer Planets," American Astronautical Society, AAS Paper 79-144, June 1979.

[12]Wallace, R. A., "Uranus Mission Options," American Astronautical Society, AAS Paper 79-145, June 1979.

[13]Wallace, R. A., "Missions to the Far Outer Planets in the 1990s," AIAA Paper 81-0311, Jan. 1981.

[14]Vaning, W., "Mercury Orbiter/Lander Using VMGA Plus Solar-Ion Propulsion," American Astronautical Society, AAS Paper 92-188, Feb. 1992.

[15]Betts, J. T., "Optimal Interplanetary Orbit Transfers by Direct Transcription," *Journal of the Astronautical Sciences*, Vol. 42, No. 3, 1994, pp. 247–268.

[16]Coverstone-Carroll, V., and Williams, S. N., "Optimal Low Thrust Trajectories Using Differential Inclusion Concepts," *Journal of the Astronautical Sciences*, Vol. 42, No. 4, 1994, pp. 379–393.

[17]Yamakawa, H., Kawaguchi, J., Uesugi, K., and Matsuo, H., "Frequent Access to Mercury in the Early 21st Century: Multiple Mercury Flyby Mission via Electric Propulsion," *Acta Astronautica*, Vol. 39, No. 1–4, 1996, pp. 133–142.

[18]Kluever, C. A., "Heliospheric Boundary Exploration Using Ion Propulsion Spacecraft," *Journal of Spacecraft and Rockets*, Vol. 34, No. 3, 1997, pp. 365–371.

[19]Kluever, C. A., "Optimal Low-Thrust Interplanetary Trajectories by Direct Method Techniques," *Journal of the Astronautical Sciences*, Vol. 45, No. 3, 1997, pp. 247–262.

[20]Sauer, C. G., "Solar Electric Performance for Medlite and Delta Class Planetary Missions," American Astronautical Society, AAS Paper 97-726, Aug. 1997.

[21]Maddock, R. W., and Sims, J. A., "Trajectory Options for Ice and Fire Preproject Missions Utilizing Solar Electric Propulsion," AIAA Paper 98-4285, Aug. 1998.

[22]Casalino, L., Colasurdo, G., and Pastrone, D., "Optimal Low-Thrust Escape Trajectories Using Gravity Assist," *Journal of Guidance, Control, and Dynamics*, Vol. 22, No. 5, 1999, pp. 637–642.

[23]Meissinger, H., F., "SEP Planetary Missions with Earth Gravity Assist Using an Initial Out-of-Ecliptic Thrust Phase," AIAA Paper 99-2869, June 1999.

[24]Colasurdo, G., and Casalino, L., "Trajectories Towards Near-Earth-Objects Using Solar Electric Propulsion," American Astronautical Society, AAS Paper 99-339, Aug. 1999.

[25]Langevin, Y., "Chemical and Solar Electric Propulsion Options for a Cornerstone Mission to Mercury," *Acta Astronautica*, Vol. 47, Nos. 2–9, 2000, pp. 443–452.

[26]Petropoulos, A. E., Longuski, J. M., and Vinh, N. X., "Shape-Based Analytic Representations of Low-Thrust Trajectories for Gravity-Assist Applications," American Astronautical Society, AAS Paper 99-337, Aug. 1999.

[27]Sims, J. A., and Flanagan, S. N., "Preliminary Design of Low-Thrust Interplanetary Missions," American Astronautical Society, AAS Paper 99-338, Aug. 1999.

[28]Petropoulos, A. E., "A Shape-Based Approach to Automated, Low-Thrust, Gravity-Assist Trajectory Design," Ph.D. Dissertation, School of Aeronautics and Astronautics, Purdue Univ., West Lafayette, IN, May 2001.

[29]Petropoulos, A. E., and Longuski, J. M., "Automated Design of Low-Thrust Gravity-Assist Trajectories," AIAA Paper 2000-4033, Aug. 2000.

[30]Petropoulos, A. E., and Longuski, J. M., "A Shape-Based Algorithm for the Automated Design of Low-Thrust, Gravity-Assist Trajectories," American Astronautical Society, AAS Paper 01-467, July–Aug. 2001.

[31]Rinderle, E. A., "Galileo User's Guide, Mission Design System, Satellite Tour Analysis and Design Subsystem," Jet Propulsion Laboratory, JPL Publ. D-263, California Inst. of Technology, Pasadena, CA, July 1986.

[32]Tsiolkovsky, K. E., "Exploration of the Universe with Reaction Machines," *Science Review*, No. 5, 1903, p. 31 (in Russian).

[33]Humble, R. W., Henry, G. N., and Larson, W. J. (eds.), "Ideal Rocket Equation," *Space Propulsion Analysis and Design*, McGraw–Hill, New York, 1995, pp. 12, 13.

[34]Kawaguchi, J., Takiura, K., and Matsuo, H., "On the Optimization and Application of Electric Propulsion to Mars and Sample and Return Mission," American Astronautical Society, AAS Paper 94-183, Feb. 1994.

[35]Brown, C. D., "Arrival Targeting," *Spacecraft Mission Design*, 2nd ed., AIAA Education Series, AIAA, Reston, VA, 1998, pp. 115–117.

[36]Gill, P. E., Murray, M., and Saunders, M. A., User's Guide for SNOPT 5.3: A FORTRAN Package for Large-Scale Nonlinear Programming," Systems Optimization Lab., Dept. of Engineering–Economic Systems and Operations Research, Stanford Univ., Stanford, CA, 1999.

[37]McConaghy, T. T., Debban, T. J., Petropoulos, A. E., and Longuski, J. M., "An Approach to Design and Optimization of Low-Thrust Trajectories with Gravity Assists," American Astronautical Society, AAS Paper 01-468, July–Aug. 2001.

[38]Whiffen, G. J., and Sims, J. A., "Application of a Novel Optimal Control Algorithm to Low-Thrust Trajectory Optimization," American Astronautical Society, AAS Paper 01-209, Feb. 2001.

C. A. Kluever
Associate Editor